Biophysical Journal Volume 73 September 1997 1440–1447

The Structure of Divalent Cation-Induced Aggregates of PIP_2 and Their Alteration by Gelsolin and Tau

Lisa A. Flanagan,* C. Casey Cunningham,* Jian Chen,# Glenn D. Prestwich,# Kenneth S. Kosik,§ and Paul A. Janmey*

*Division of Experimental Medicine, Department of Medicine, Brigham and Women's Hospital and Harvard Medical School, Boston, Massachusetts 02115; #Department of Medicinal Chemistry, University of Utah, Salt Lake City, Utah 84112; and §Department of Neurology, Center for Neurologic Diseases, Brigham and Women's Hospital and Harvard Medical School, Boston, Massachusetts 02115 USA

ABSTRACT Phosphatidylinositol bisphosphate (PIP_2) serves as a precursor for diacylglycerol and inositol trisphosphate in signal transduction cascades and regulates the activities of several actin binding proteins that influence the organization of the actin cytoskeleton. Molecules of PIP_2 form 6-nm diameter micelles in water, but aggregate into larger, multilamellar structures in physiological concentrations of divalent cations. Electron microscopic analysis of these aggregates reveals that they are clusters of striated filaments, suggesting that PIP_2 aggregates form stacks of discoid micelles rather than multilamellar vesicles or inverted hexagonal arrays as previously inferred from indirect observations. The distance between striations within the filaments varies from 4.2 to 5.4 nm and the diameter of the filaments depends on the dehydrated ionic radius of the divalent cation, with average diameters of 19, 12, and 10 nm for filaments formed by Mg^{2+}, Ca^{2+}, and Ba^{2+}, respectively. The structure of the divalent cation-induced aggregates can be altered by PIP_2 binding proteins. Gelsolin and the microtubule associated protein tau both affect the formation of aggregates, indicating that tau acts as a PIP_2 binding protein in a manner similar to gelsolin. In contrast, another PIP_2 binding protein, profilin, does not modify the aggregates.

INTRODUCTION

Phosphatidylinositol bisphosphate (PIP_2) plays a critical role in cellular signaling and binds to several intracellular proteins. The best-studied function of inositol lipids is the hydrolysis of $PI(4,5)P_2$ by phospholipase C (PLC) to form diacylglycerol and inositol trisphosphate, which lead, respectively, to the activation of protein kinase C and increased cytosolic calcium. The synthesis of both $PI(3,4)P_2$ and $PI(4,5)P_2$ by phosphoinositide kinases and phosphatases is stimulated by activation of cell surface receptors, and the formation of these lipids may have signaling roles independent of or synergistic with those regulated by PLC (Divecha and Irvine, 1995; Kapeller and Cantley, 1994). The importance of the latter signaling mechanisms may relate to the numerous findings that PIP_2 binds to and regulates the activities of several actin binding proteins, and may thereby influence the organization of the cytoskeleton (Hartwig et al., 1995; for review see Janmey, 1994).

PIP_2 forms 6-nm diameter micelles in neutral, low ionic strength aqueous solutions (Hirai et al., 1996; Sugiura, 1981). Divalent cations bind PIP_2 through its negatively charged headgroup and at millimolar concentrations induce the formation of large, multilamellar PIP_2 aggregates (Fullington and Hendrickson, 1966; Hendrickson and Fullington, 1965; Hirai et al., 1996). This ability to aggregate PIP_2 depends on formation of ionic bonds rather than screening of electrostatic repulsions, since PIP_2 remains micellar in concentrations of monovalent cations >100 mM (Hirai et al., 1996). The structure of PIP_2 aggregates has not been described, but aggregates of other lipids form planar sheets, inverted hexagonal arrays, or large bilayer vesicles (Fuhrhop and Helfrich, 1993; Rupert et al., 1987).

In vitro studies of PIP_2 are often done in the presence of millimolar concentrations of divalent cations to aggregate the lipid into a membranous structure and mimic the intracellular levels of Mg^{2+}. Lipid aggregate structures vary in the extent to which they expose phospholipid headgroups to the aqueous environment, and since many PIP_2 binding proteins interact with the headgroup, the structure of PIP_2 aggregates can affect protein binding (Goldschmidt-Clermont et al., 1990; Lassing and Lindberg, 1985). Therefore, analysis of the structure of PIP_2 aggregates can predict how headgroup exposure is affected by aggregation.

Using electron microscopy and light scattering, this study describes the morphology of aggregates of PIP_2 produced by the divalent cations Mg^{2+}, Ca^{2+}, and Ba^{2+}. In addition, since the binding of PIP_2 to intracellular proteins may alter the micellar structure or surface charge of the lipid, the effect of phospholipid-protein binding on aggregation was investigated using two actin binding proteins, gelsolin and profilin, and the microtubule associated protein tau. Actin polymerization can be triggered when gelsolin and profilin are dissociated from actin by PIP_2, which is the only physiological stimulus that can perform this function (Goldschmidt-Clermont et al., 1990; Janmey et al., 1987; Janmey and Stossel, 1987; Lassing and Lindberg, 1985). The interaction of these actin binding proteins with PIP_2 has been extensively characterized in vitro, making these proteins ideal candidates to study the effect of protein binding on

Received for publication 10 December 1996 and in final form 2 June 1997.

Address reprint requests to Lisa A. Flanagan, Ph.D., Division of Experimental Medicine, Brigham and Women's Hospital, 221 Longwood Ave. – LMRC 312, Boston, MA 02115. Tel.: 617-278-0326; Fax: 617-734-2248; E-mail: flanagan@calvin.bwh.harvard.edu.

0006-3495/97/09/1440/08 $2.00

PIP_2 aggregation. Tau can associate with the plasma membrane in cultured cells and, in addition to the microtubule associated proteins MAP2 and MAP2c, interacts in vitro with phosphatidylinositol (PI) (Brandt et al., 1995; Surridge and Burns, 1994). These results raise the possibility that tau binds other phospholipids, such as PIP_2.

MATERIALS AND METHODS

Reagents and protein purification

PI(4,5)P_2 (Sigma, St. Louis, MO) was hydrated in 10 mM tris, pH 7.4 to 0.5 mg/ml and sonicated as previously described (Janmey and Stossel, 1989). The purity of PI(4,5)P_2 and phosphatidylcholine (PC) (Sigma, St. Louis, MO) was confirmed by thin layer chromatography (Ling et al., 1989). NBD-labeled PIP_2 was synthesized as previously described (Chen et al., 1996). Recombinant human plasma gelsolin purified from bacteria was kindly provided by Blake Pepinsky, Biogen Inc., Cambridge, MA. Calf spleen profilin was purified as described (Janmey, 1991). The human three-repeat isoform of tau was expressed in Sf9 cells as previously described (Knops et al., 1991). Tau was initially purified by adjusting the supernatant from cells to 0.75 M NaCl and 2% βME and boiling for 10 min to precipitate nearly all contaminating cellular proteins. Soluble, heat-stable tau was separated by centrifugation, dialyzed against 10 mM tris, pH 8.0, and loaded onto a Mono Q FPLC column. Tau is variably phosphorylated in Sf9 cells and gains enough negative charge to bind to Mono Q. Purified tau eluted at ~400 mM KCl. For control experiments, samples were identically purified from Sf9 cells infected with wild-type virus. Purified samples from these cells contained no tau protein as detected by Western blotting with a monoclonal antibody to tau (5E2) (Kosik et al., 1988).

Light scattering

Light scattering intensity was measured with a Brookhaven Instruments BI30AT apparatus. The incident light was a 633-nm beam from a 10-mW helium-neon laser, and scattered light was collected for 1 min at a 90° angle. The average size of PIP_2 aggregates was estimated from a cumulant fit to the intensity autocorrelation function using standard methods (Berne and Pecora, 1976). Various concentrations of divalent cations ($MgCl_2$, $CaCl_2$, or $BaCl_2$) were added to 15 μM (17 μg/ml) PIP_2 in 10 mM tris, pH 7.4, and the scattering measured after a 10-min incubation. In some cases, monovalent salts (120 mM NaCl or KCl) or proteins (2 μM gelsolin, profilin, or tau) were added to PIP_2 before the addition of divalent cations.

Electron microscopy

Samples used for light scattering studies (see above) were attached to carbon films, negatively stained, and observed by electron microscopy (EM). Carbon films were prepared by evaporating carbon onto a freshly cleaved mica surface. The carbon films were floated off the mica onto samples, then rinsed with 10 mM tris, pH 7.4 buffer, and stained with 2% uranyl acetate in H_20 (Lake, 1979). The stained carbon films were picked up onto formic acid-washed carbon mesh grids, and the grids were observed in a JEOL-1200EX electron microscope at 100 kV.

Fluorescence microscopy

Fluorescently labeled PC/PIP_2 vesicles (9:1 PC/PIP_2) were prepared by mixing chloroform solutions of PC and NBD-labeled PIP_2, evaporating the chloroform mixture onto a glass surface, and rehydrating the lipids in 10 mM tris, pH 7.4. Fluorescently labeled aggregates of PIP_2 were formed from mixed micelles containing 9:1 unlabeled/labeled PIP_2, which were generated by sonicating PIP_2 and NBD-PIP_2 micelles in 10 mM tris, pH 7.4 to redistribute the lipids. Vesicles and aggregates were observed on a fluorescence microscope (Nikon) and images captured into National Institutes of Health Image 1.6.

Quantitation of dimensions of PIP_2 aggregates

Electron micrographs of negatively stained PIP_2 aggregates were digitized using an Avec scanner and the Adobe Photoshop software program, and transferred into National Institutes of Health Image 1.6. The scanned scale bar from the micrograph was used to calibrate the measurement scale in Image and measurements of the width of the individual filaments and spacing between striations made with the Image program. Each individual filament in a sample has inherent variability along its length, especially for width. In order to compare among samples, the average width of each filament was obtained from 10–20 measurements along that filament. The averages of several randomly selected filaments in a sample were used to obtain an average and standard deviation for that sample. These values were then used to compare among samples. The same strategy was used for comparing striations. Spacing between striations refers to the distance between electron-dense bands along an individual filament. In this case, the average striation spacing was measured by determining the distance between 10–20 electron-dense bands in a filament and then averaging the values from several randomly selected filaments to obtain the mean and standard deviation for spacing between striations in that sample.

Analysis of tau-PIP_2 binding

The binding of tau to PIP_2 aggregates was quantified by incubating varying concentrations of tau (2.5–10 μM) with 10 μM PIP_2, then adding 1 mM Ca^{2+} to aggregate the PIP_2/tau complexes. Aggregates were pelleted (100,000 *g*, 1 h, 25°C) and the concentration of tau determined in the supernatant and pellet by densitometric analysis of Coomassie stained tau bands on polyacrylamide gels. Tau does not pellet in the presence of 1 mM Ca^{2+} without PIP_2, and light scattering showed that virtually all PIP_2 aggregates sediment.

RESULTS

Aggregates of PIP_2 induced by divalent cations are clusters of striated filaments

The aggregation of PIP_2 by divalent cations was monitored by light scattering and the average size of the aggregates in solution estimated by an intensity autocorrelation function (Berne and Pecora, 1976). Light scattering from low concentrations of PIP_2 (15 μM in 10 mM tris buffer) was only slightly greater than from buffer alone, confirming that PIP_2 exists as small micelles in the absence of divalent cations (Sugiura, 1981). Addition of Mg^{2+}, Ca^{2+}, or Ba^{2+} aggregated PIP_2 into larger structures as detected by increased light scatter from these samples compared to PIP_2 alone (Fig. 1). The differences in scattering intensity were consistent with estimates of the average particle diameters of aggregates, which were 1310 nm for Mg^{2+}, 1180 nm for Ca^{2+}, and 1000 nm for Ba^{2+}. The aggregation of PIP_2 by divalent cations is reversible, since 10 mM EDTA or EGTA disrupted the aggregates (data not shown). The formation of PIP_2 aggregates required divalent cations, as 120 mM NaCl or KCl neither increased the light scatter of PIP_2 samples nor produced any structures visible by EM. This is in agreement with previous studies using x-ray scattering to show that Ca^{2+} and Mg^{2+} induce larger aggregates of PIP_2,

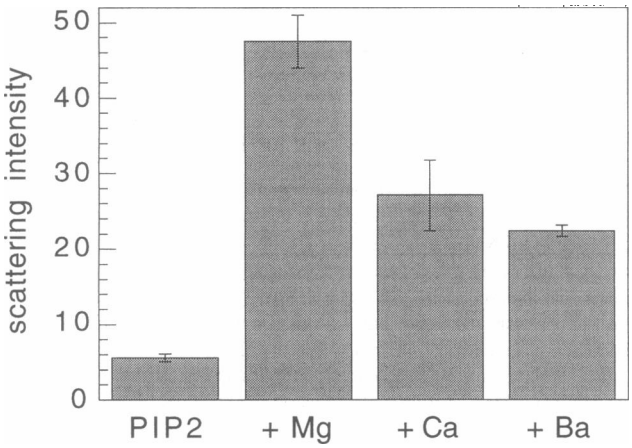

FIGURE 1 Divalent cations increased light scattering from PIP_2. Addition of 1 mM Mg^{2+}, Ca^{2+}, or Ba^{2+} greatly increased the light scattering intensity of solutions containing 15 μM PIP_2. Scattering intensity is the average intensity from at least 10 measurements for each divalent cation and is expressed in arbitrary units.

while Na^+ does not (Hirai et al., 1996). Aggregation of PIP_2 by divalent cations was not affected by the concurrent addition of 120 mM NaCl or KCl (Fig. 6 *e* and data not shown).

The PIP_2 aggregates induced by all three divalent cations were shown by negative staining to be clusters of striated filaments (Fig. 2). The aggregates pictured are particularly large in order to more clearly show the structure. Similar filamentous structures were observed by EM of rotary shadowed PIP_2 aggregates, although the striated pattern was not visible (data not shown). In order to ensure that these structures were not a result of the drying and staining involved in preparing the samples for EM, fluorescently labeled PIP_2 aggregates were observed in the light microscope. These aggregates were formed from micelles containing 10% NBD-labeled PIP_2 and were compared to large, multilamellar vesicles made up of 90% PC and 10% NBD-labeled PIP_2 (Chen et al., 1996; Prestwich, 1996). Aggregates containing fluorescently labeled PIP_2 had the same morphology by negative staining EM as unlabeled aggregates (data not shown). Fluorescence microscopy showed that the labeled aggregates in solution were clusters of filaments reminiscent of the structures seen by EM (Fig. 3). An especially large aggregate is pictured in order to clearly show the structure, since all the visible aggregates in the sample had the same structure regardless of size. The morphology of the aggregates did not resemble multilamellar vesicles such as those formed by PC/PIP_2 mixtures.

Analysis of the electron micrographs of the negatively stained PIP_2 aggregates revealed that the dimensions of the filaments depended on the divalent cation (Table 1). The widest filaments were formed by Mg^{2+} and the thinnest by Ba^{2+}. Addition of monovalent cations tended to decrease the width of the filaments, but this effect was only significant with KCl. The spacing between striations in the filaments varied slightly with the species of divalent cation

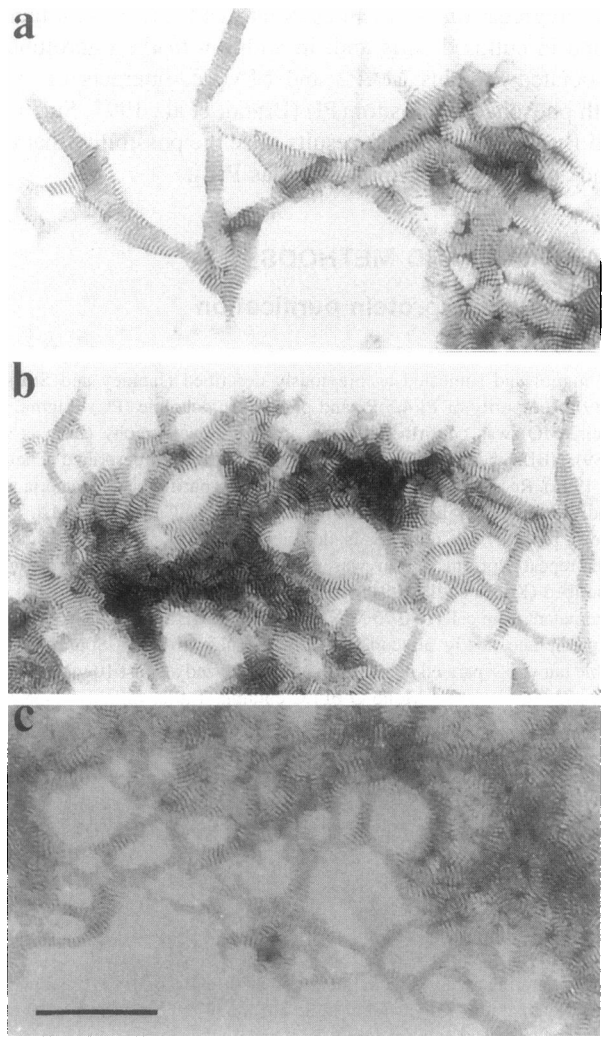

FIGURE 2 PIP_2 aggregated with divalent cations formed clusters of striated filaments. Samples containing 15 μM PIP_2 and 1 mM (*a*) Mg^{2+}, (*b*) Ca^{2+}, or (*c*) Ba^{2+} were examined by negative staining EM, scale bar = 100 nm. PIP_2 without divalent cations showed no structure discernible by negative staining.

used to form the aggregates, in the order $Ba^{2+}>Mg^{2+}>Ca^{2+}$ (Table 1). Inclusion of monovalent cations slightly increased the distance between the striations.

The threshold for aggregation of PIP_2 was 100 μM divalent cation, and higher concentrations up to 1 mM increased the number and clustering of striated filaments (Fig. 4). Both Mg^{2+} and Ba^{2+} gave 50% maximal scatter at 300 μM concentrations and a gradual increase in PIP_2 aggregation between 100 and 800 μM (Fig. 4 *a*). In contrast, the concentration of Ca^{2+} required for 50% maximal scatter was 112 μM and formation of PIP_2 aggregates increased sharply between 100 and 150 μM (Fig. 4 *a*). Electron micrographs of negatively stained PIP_2 aggregates showed that those induced by low concentrations of Mg^{2+} were thin and short and that higher concentrations of divalent cation resulted in wider and longer filaments that eventually become tortuous and clustered (Fig. 4, *b–g*). Between 0.1 and

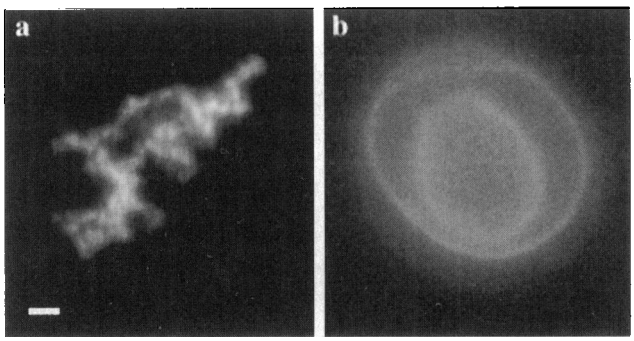

FIGURE 3 Aggregates of PIP_2 observed by fluorescence microscopy were clusters of filaments rather than multilamellar vesicles. Samples of fluorescent lipids were sealed between a glass slide and coverslip to observe the lipids in solution: (*a*) 10% NBD-labeled PIP_2 micelles aggregated with 1 mM Ca^{2+}, (*b*) 90% PC/10% NBD-labeled PIP_2 vesicles. Scale bar = (*a*) 1 μm, (*b*) 1.4 μm.

0.2 mM Mg^{2+} the filaments increased in width and length, whereas between 0.2 and 1.0 mM Mg^{2+} the filaments increased in length and clustering without a change in width.

Gelsolin and tau alter the structure of PIP_2 aggregates

PIP_2 was incubated with gelsolin, profilin, or tau before addition of divalent cations to determine whether protein binding has an effect on the aggregation of PIP_2. In the absence of divalent cations these proteins produced no lipid aggregates detectable by light scattering or EM. However, incubation of PIP_2 with gelsolin before aggregation with Mg^{2+} produced thinner and less clustered filaments than those formed by Mg^{2+} alone (Fig. 5, *a* and *b*). In contrast, profilin had no effect on the aggregated structure produced by Mg^{2+} (Fig. 5 *c*). Tau altered aggregate formation by forming short, thin, single striated filaments that were much smaller and less clustered than those produced by Mg^{2+} alone (Fig. 5 *d*). Light scattering from these aggregates gave an estimated average diameter of 170 nm, which is much smaller than the average diameter of aggregates formed by Mg^{2+} alone (1310 nm). Glutathione S-transferase, a protein that does not bind PIP_2 and thus serves as a negative control, had no effect on the aggregated PIP_2 structures produced by Mg^{2+} (data not shown).

TABLE 1 The species of divalent cation and presence of monovalent cation often influenced the width and spacing between striations of the filaments

Cation	Width (nm)	Striation Spacing (nm)
Mg^{2+}	18.7 ± 0.7	5.0 ± 0.4
Ca^{2+}	11.6 ± 0.6	4.2 ± 0.1
+NaCl	10.3 ± 1.1	5.0 ± 0.1
+KCl	9.5 ± 0.3	4.8 ± 0.2
Ba^{2+}	9.7 ± 0.9	5.4 ± 0.1

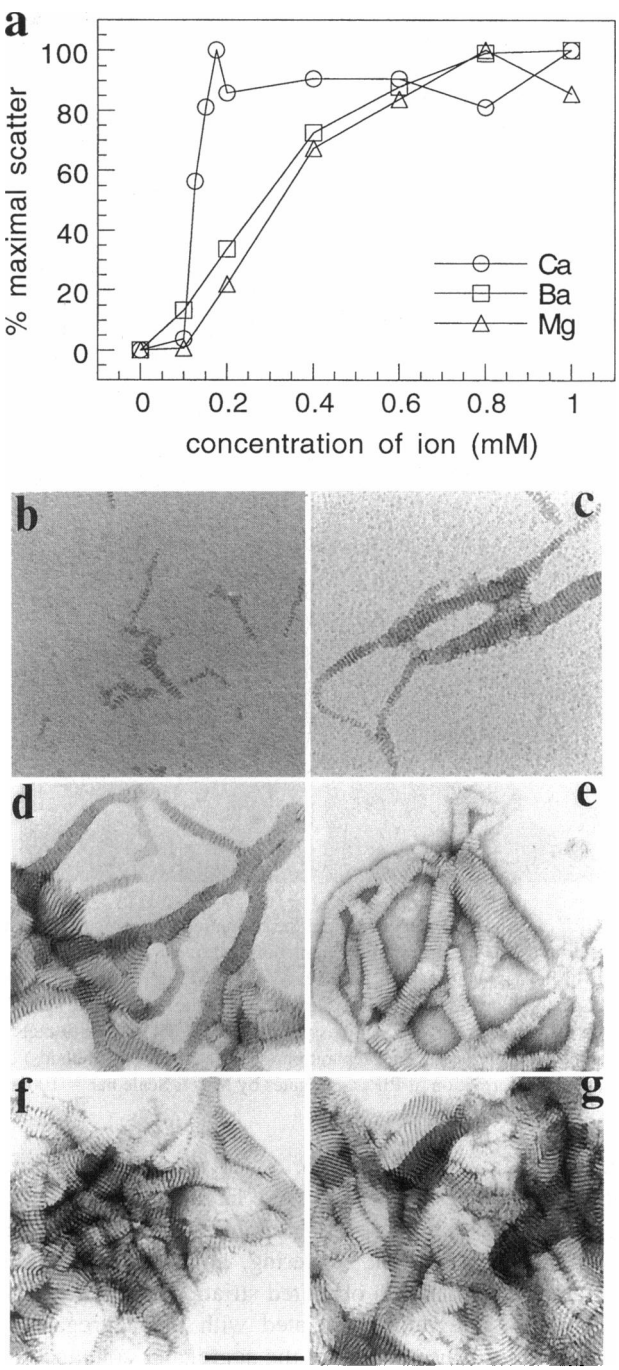

FIGURE 4 The formation of aggregates of PIP_2 was dependent on the concentration of divalent cation. (*a*) light scattering intensity was used to monitor the formation of aggregates of PIP_2 (15 μM) in the presence of varying concentrations of divalent cations. The data are expressed as percent maximal scatter with 100% representing the maximum scatter for each individual cation. (*b–g*) a representative series of electron micrographs of 15 μM PIP_2 in varying concentrations of Mg^{2+} show the development of PIP_2 aggregates. Concentrations of Mg^{2+} were (*b*) 0.1 mM, (*c*) 0.2 mM, (*d*) 0.4 mM, (*e*) 0.6 mM, (*f*) 0.8 mM, and (*g*) 1.0 mM. Scale bar = 100 nm.

Gelsolin obscured the striated pattern of the filaments in Ca^{2+}-induced aggregates of PIP_2 (Fig. 6 *b*), whereas profilin produced no clear difference from the aggregates in-

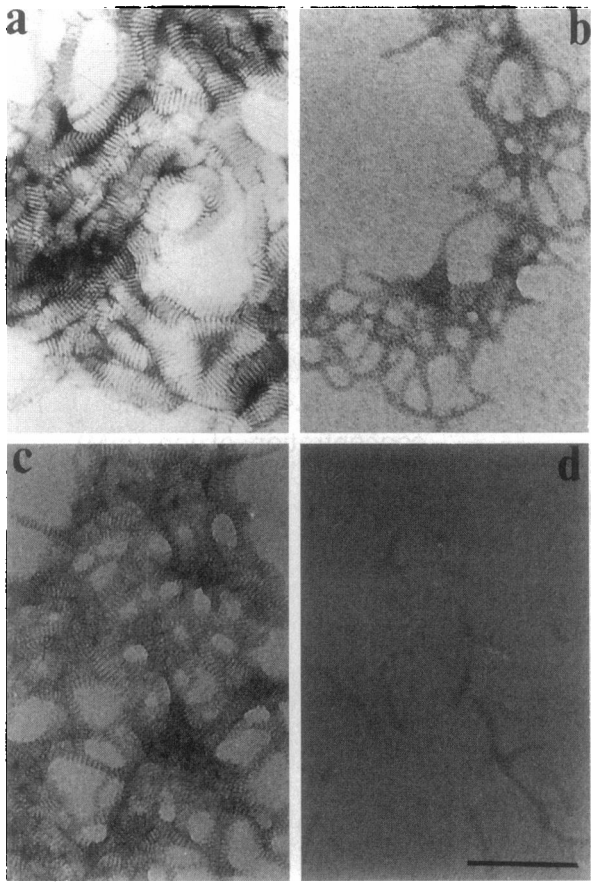

FIGURE 5 Gelsolin and tau altered the formation of aggregates of PIP_2 induced by Mg^{2+}. Electron micrographs of negatively stained samples of 15 μM PIP_2 aggregated with 1 mM Mg^{2+} or 1 mM Mg^{2+} after addition of 2 μM gelsolin, profilin, or tau: (*a*) Mg^{2+}, (*b*) gelsolin + Mg^{2+}, (*c*) profilin + Mg^{2+}, (*d*) tau + Mg^{2+}. Samples prepared from wild-type Sf9 cells as negative controls for the tau preparation (see Materials and Methods) did not affect the formation of PIP_2 aggregates by Mg^{2+}. Scale bar = 100 nm.

duced by Ca^{2+} alone (Fig. 6, *a* and *c*). PIP_2 aggregates formed in the presence of tau were larger in average diameter (1990 nm) than those formed by Ca^{2+} alone (1180 nm) as estimated from light scattering, and contained highly clustered filaments with obscured striations (Fig. 6 *d*). Tau protein was integrally associated with the aggregates in these samples, since pellets of the aggregates contained tau (Fig. 7). Tau also altered the formation of PIP_2 aggregates by Ca^{2+} in the presence of 120 mM NaCl or KCl. The monovalent salts did not disturb the formation of aggregates by the divalent cation, but the presence of tau induced the formation of smaller, single thin filaments rather than a large aggregated structure (Fig. 6, *e* and *f*, and data not shown). The average diameter of these aggregates deduced from light scattering was 130 nm as compared to 1050 nm average diameter of Ca^{2+}/NaCl-induced aggregates.

The affinity of tau for PIP_2 can be roughly estimated using the fact that tau, which is normally soluble, pellets with aggregates of PIP_2 formed by Ca^{2+}. A Scatchard plot analysis of the data shows that at lower tau concentrations (1.3–2 μM bound) the apparent K_d is 0.8 μM and the

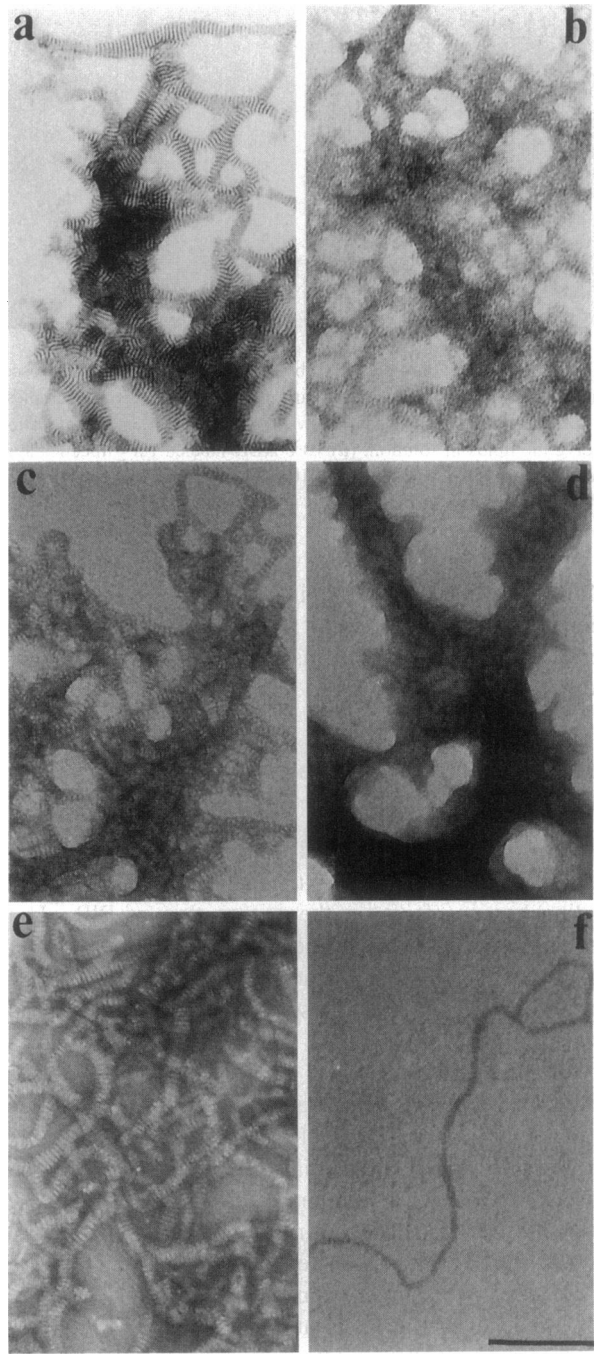

FIGURE 6 PIP_2 aggregates formed by Ca^{2+} were altered by gelsolin and tau. Electron micrographs of negatively stained samples of 15 μM PIP_2 aggregated with 1 mM Ca^{2+} or 1 mM Ca^{2+} after addition of 2 μM gelsolin, profilin, or tau: (*a*) Ca^{2+}, (*b*) gelsolin + Ca^{2+}, (*c*) profilin + Ca^{2+}, (*d*) tau + Ca^{2+}, (*e*) 1 mM Ca^{2+} and 120 mM NaCl, (*f*) 2 μM tau + 1 mM Ca^{2+} and 120 mM NaCl. Similar results were obtained with 120 mM KCl. Samples prepared from Sf9 cells as negative controls for the tau preparation (see Materials and Methods) produced no effect on PIP_2 aggregation. Scale bar = 100 nm.

binding stoichiometry is 1:4.3 tau/PIP_2 (Fig. 7). At higher tau concentrations (2.2–3.1 μM bound) the estimated K_d is 4.8 μM, representing either a different, low affinity binding site or a nonspecific interaction of PIP_2 with tau. The K_d for

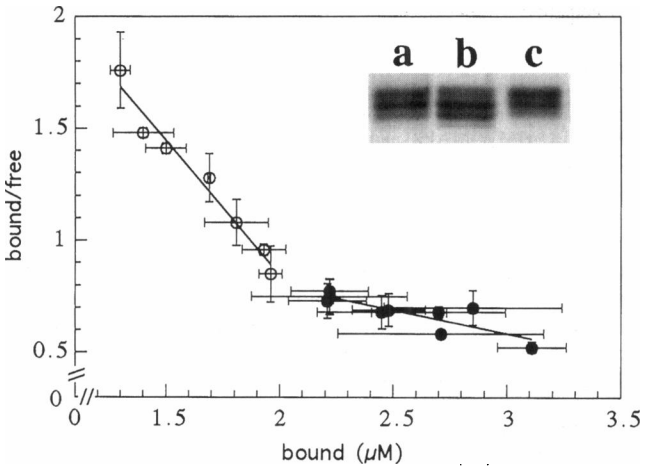

FIGURE 7 Analysis of tau-PIP_2 binding showed two distinct affinities. The binding of varying concentrations of tau to 10 μM PIP_2 was analyzed by a Scatchard plot. The binding assay was as described (see Materials and Methods). The linear curve fit for the open circles gave R = 0.98 and K_d 0.8 μM and for closed circles gave R = 0.84, K_d 4.8 μM. The mean and standard deviation represent at least three separate experiments. Inset: Coomassie stained gel of representative samples from the binding assay: (*a*) total tau, (*b*) tau in the pellet, (*c*) tau in the supernatant.

the higher affinity binding may be an underestimate, since it appears that only a subset of the tau used in the assay interacts with PIP_2. Tau expressed in Sf9 cells is variably phosphorylated, resulting in a range of phosphorylated species with isoelectric points from 6.5 to 8 (data not shown). These phosphorylated isoforms can be visualized as a series of bands on 1-D gels, with the more phosphorylated species showing slower mobility. An analysis of the tau in the supernatants and pellets showed a tendency for the less phosphorylated species to be preferentially in the pellet, or bound fraction, and the higher phosphorylated forms in the supernatant (Fig. 7, *inset*).

DISCUSSION

This study describes the morphology of divalent cation-induced aggregates of PIP_2 and the influence of three proteins on these structures. Based on the regular 5-nm spacing of the striations in the filaments, which is consistent with the dimensions of a single lipid bilayer and smaller than a 6-nm spherical PIP_2 micelle, and the expectation that divalent cations will bridge the negatively charged phospholipid headgroups, these structures are interpreted as stacks of discoid micelles of PIP_2. This interpretation is consistent with the multilamellar array and 5.7-nm spacing predicted by x-ray scattering of PIP_2 aggregates (Hirai et al., 1996). Previous EM studies of lipid aggregates using negative staining have demonstrated that stacks of disks are formed by other types of lipids. For example, mixtures of lysolecithin (PC with a single acyl chain) and PC variants containing different acyl chains were able to form stacks of disks (Inoue et al., 1977). Also, PC plus an edge-stabilizing detergent can, after extensive sonication, form stacks of disks that after several hours fuse to form unilamellar vesicles (Fromherz et al., 1986). Both of these cases utilized two different lipid species and suggested that a mixture of lipids is required to stabilize the edge of the disks and protect the hydrophobic interior from exposure to the aqueous environment (Fuhrhop and Helfrich, 1993). However, aggregation of PIP_2 with divalent cations produced a stacked disk structure from a single lipid species with two acyl chains, possibly because the curvature stabilized by the large PIP_2 headgroup minimizes the edge energy of the cylindrical stacks. Another phospholipid with a negatively charged headgroup, phosphatidylserine, also aggregates with calcium but the structure appears to be a planar sheet that rolls into a cylindrical, multilamellar structure (Papahadjopoulos et al., 1975).

The width of the micelle stacks decreased in the order $Mg^{2+}>Ca^{2+}>Ba^{2+}$, suggesting that the smaller the dehydrated (ionic) diameter of the cation, the greater the radius of curvature of the discoid micelle. These results fit with previous predictions that the aggregation of PIP_2 involves dehydration of the headgroup, allowing tighter packing of the headgroups and the formation of a flatter edge along the micelle (Hirai et al., 1996). The ability of divalent cations to increase the packing of PIP_2 headgroups may explain the formation of lateral domains of PIP_2 in phospholipid vesicles by a polybasic peptide from MARCKS (Glaser et al., 1996). Consistent with previous data, Ca^{2+} has a higher affinity for PIP_2 than Mg^{2+} and more efficiently induced aggregation (Hirai et al., 1996). This effect of Ca^{2+} suggests that small increases in local concentrations of Ca^{2+} may affect the structure of nearby pools of PIP_2 by inducing tighter packing of the headgroups, thus increasing the radius of curvature of the membrane in that region.

The stacked disk structure of PIP_2 aggregates greatly reduces the number of headgroups exposed to the aqueous environment, which would reduce the binding of proteins that rely on the headgroup for their interaction with PIP_2. This effect may explain why aggregation of PIP_2 with divalent cations reduced the effects of the phospholipid on gelsolin function in a previous study (Janmey et al., 1987). Gelsolin and profilin are both PIP_2 binding proteins, but gelsolin altered the formation of PIP_2 aggregates while profilin did not, perhaps reflecting differences in the binding of these two proteins to PIP_2. Previous studies suggested that the binding is not equivalent, since concentrations of >500 nM profilin are required to disrupt the binding of 30 nm gelsolin to 11 μM PIP_2 (Janmey and Stossel, 1989). Gelsolin and profilin bind to PIP_2 with similar stoichiometries (1:8 gelsolin/PIP_2 and 1:7 profilin/PIP_2) and both utilize positively charged regions of the protein to bind to the negatively charged headgroup of PIP_2 (Federov et al., 1994; Goldschmidt-Clermont et al., 1990; Janmey et al., 1992; Yu et al., 1992). Therefore, they may differ in affinity for PIP_2 or the extent to which a hydrophobic component contributes to the binding.

The fact that tau alters the structure of aggregates of PIP_2 induced by two different species of divalent cations suggests that tau is a PIP_2 binding protein. The K_d for this interaction is ~0.8 μM, which suggests that these molecules could bind in vivo since the intracellular concentration of PIP_2 is ~100–300 μM and tau is ~5–10 μM (Ferreira et al., 1989; Rittenhouse and Sasson, 1985). Tau can also bind PIP_2 in a PC bilayer, suggesting that the micellar structure of PIP_2 is not necessary for the interaction (W. Foster and P.A. Janmey, personal communication). Tau interacts with arachidonic acid and may therefore associate hydrophobically with the acyl chains of PIP_2, one of which is arachidonic acid (Wilson and Binder, 1995). However, tau also binds to dipalmitoyl $PI(3,4)P_2$ that lacks arachidonic acid, so the effect of tau on PIP_2 aggregation is not due specifically to the presence of arachidonic acid (data not shown). Binding of tau to PIP_2 may relate to recent data showing that a subset of non-microtubule bound tau interacts with the plasma membrane in cultured cells (Brandt et al., 1995). Tau has also been found in the nucleus, a site of PIP_2 accumulation in cells (Divecha et al., 1993; Thurston et al., 1996; Wang et al., 1993). A recent study shows that tau can enhance the cleavage of PIP_2 by PLCγ, an effect that is potentiated by arachidonic acid (Hwang et al., 1996). The data presented here suggest that this effect may be due to direct binding of tau to PIP_2 to make it a more favorable substrate for PLCγ.

This study describes the structure of divalent cation-induced aggregates of PIP_2 and shows that a single lipid species with two acyl chains can form stacks of discoid micelles. The interaction of PIP_2 with specific proteins can alter the formation of aggregates by divalent cations, an effect that also depends on the species of divalent cation. In addition, the results presented here indicate that the microtubule associated protein tau binds to PIP_2, an association that may affect the function of tau and PIP_2 intracellularly.

We are thankful to John Hartwig for instruction in electron microscopy and Ueli Aebi for many helpful discussions.

This work was supported by NIH grants HL07680, GM18859, NS29031, NS29632, and AR38910.

REFERENCES

Berne, B., and R. Pecora. 1976. Dynamic Light Scattering. John Wiley & Sons, New York.

Brandt, R., J. Leger, and G. Lee. 1995. Interaction of tau with the neural plasma membrane mediated by tau's amino-terminal projection domain. *J. Cell Biol.* 131:1327–1340.

Chen, J., A. A. Profit, and G. D. Prestwich. 1996. Synthesis of photoactivatable 1,2-o-diacyl-sn-glycerol derivatives of 1-l-phosphatidyl-d-myo-inositol 4,5-bisphosphate (ptdinsp(2)) and 3,4,5-trisphosphate (ptdinsp(3)). *J. Org. Chem.* 61:6305–6312.

Divecha, N., H. Banfic, and R. F. Irvine. 1993. Inositides and the nucleus and inositides in the nucleus. *Cell.* 74:405–407.

Divecha, N., and R. F. Irvine. 1995. Phospholipid signaling. *Cell.* 80: 269–278.

Federov, A. A., K. A. Magnus, M. H. Graupe, E. E. Lattman, T. D. Pollard, and S. C. Almo. 1994. X-ray structure of isoforms of the actin binding protein profilin that differ in their affinity for polyphosphoinositides. *Proc. Natl. Acad. Sci. U.S.A.* 91:8636–8640.

Ferreira, A., J. Busciglio, and A. Caceres. 1989. Microtubule formation and neurite growth in cerebellar macroneurons which develop in vitro: evidence for the involvement of the microtubule-associated proteins, MAP-1a, HMW-MAP2 and Tau. *Brain Res. Dev. Brain Res.* 49: 215–228.

Fromherz, P., C. Rocker, and D. Ruppel. 1986. From discoid micelles to spherical vesicles—the concept of edge activity. *Farad Disc. Chem. Soc.* 81:39–48.

Fuhrhop, J.-H., and W. Helfrich. 1993. Fluid and solid fibers made of lipid molecular bilayers. *Chem. Rev.* 93:1565–1582.

Fullington, J. G., and H. S. Hendrickson. 1966. Phospholipid-metal complexes. Interaction of triphosphoinositide- and phosphatidylserine-metal complexes with ethylenediamine, polyaminoacids, and protein. *J. Biol. Chem.* 241:4098–4100.

Glaser, M., S. Wanaski, C. A. Buser, V. Boguslavsky, W. Rashidzada, A. Morris, M. Rebecchi, S. F. Scarlata, L. W. Runnels, G. D. Prestwich, J. Chen, A. Aderem, J. Ahn, and S. McLaughlin. 1996. Myristoylated alanine-rich C kinase substrate (MARCKS) produces reversible inhibition of phospholipase C by sequestering phosphatidylinositol 4,5-bisphosphate in lateral domains. *J. Biol. Chem.* 271:26187–26193.

Goldschmidt-Clermont, P. J., L. M. Machesky, J. J. Baldassare, and T. D. Pollard. 1990. The actin-binding protein profilin binds to PIP2 and inhibits its hydrolysis by phospholipase C. *Science.* 247:1575–1578.

Hartwig, J. H., G. M. Bokoch, C. L. Carpenter, P. A. Janmey, L. A. Taylor, A. Toker, and T. P. Stossel. 1995. Thrombin receptor ligation and activated Rac uncap actin filament barbed ends through phosphoinositide synthesis in permeabilized human platelets. *Cell.* 82:643–653.

Hendrickson, H. S., and J. G. Fullington. 1965. Stabilities of metal complexes of phospholipids: Ca(II), Mg(II), and Ni(II) complexes of phosphatidylserine and triphosphoinositide. *Biochem.* 4:1599–1605.

Hirai, M., T. Takizawa, S. Yabuki, Y. Nakata, T. Hirai, and K. Hayashi. 1996. Salt-dependent phase behavior of the phosphatidylinositol 4,5-diphosphate-water system. *J. Chem. Soc., Farad Trans.* 92:1493–1498.

Hwang, S., D.-Y. Jhon, Y. Bae, J. Kim, and S. Rhee. 1996. Activation of phospholipase C-gamma by the concerted action of tau proteins and arachidonic acid. *J. Biol. Chem.* 271:18342–18349.

Inoue, K., K. Suzuki, and S. Nojima. 1977. Morphology of lipid micelles containing lysolecithin. *J. Biochem.* 81:1097–1106.

Janmey, P. 1994. Phosphoinositides and calcium as regulators of cellular actin assembly and disassembly. *Ann. Rev. Physiol.* 56:169–191.

Janmey, P. A. 1991. Polyproline affinity method for purification of platelet profilin and modification with pyrene-maleimide. *Methods Enzymol.* 196:92–99.

Janmey, P. A., K. Iida, H. L. Yin, and T. P. Stossel. 1987. Polyphosphoinositide micelles and polyphosphoinositide-containing vesicles dissociate endogenous gelsolin-actin complexes and promote actin assembly from the fast-growing end of actin filaments blocked by gelsolin. *J. Biol. Chem.* 262:12228–12236.

Janmey, P. A., J. Lamb, P. G. Allen, and P. T. Matsudaira. 1992. Phosphoinositide-binding peptides derived from the sequences of gelsolin and villin. *J. Biol. Chem.* 267:11818–11823.

Janmey, P. A., and T. P. Stossel. 1987. Modulation of gelsolin function by phosphatidylinositol 4,5-bisphosphate. *Nature.* 325:362–364.

Janmey, P. A., and T. P. Stossel. 1989. Gelsolin-polyphosphoinositide interaction. Full expression of gelsolin-inhibiting function by polyphosphoinositides in vesicular form and inactivation by dilution, aggregation, or masking of the inositol head group. *J. Biol. Chem.* 264:4825–4831.

Kapeller, R., and L. C. Cantley. 1994. Phosphatidylinositol 3-kinase. *Bioessays.* 16:565–576.

Knops, J., K. S. Kosik, G. Lee, J. D. Pardee, L. Cohen-Gould, and L. McConlogue. 1991. Overexpression of tau in a nonneuronal cell induces long cellular processes. *J. Cell Biol.* 114:725–733.

Kosik, K. S., L. D. Orecchio, L. Binder, J. Q. Trojanowski, V. M. Lee, and G. Lee. 1988. Epitopes that span the tau molecule are shared with paired helical filaments. *Neuron.* 1:817–825.

Lake, J. A. 1979. Practical aspects of immune electron microscopy. *Methods Enzymol.* 61:250–257.

Lassing, I., and U. Lindberg. 1985. Specific interaction between phosphatidylinositol 4,5-bisphosphate and profilactin. *Nature.* 314:472–474.

Ling, L. E., J. T. Schulz, and L. C. Cantley. 1989. Characterization and purification of membrane-associated phosphatidylinositol-4-phosphate kinase from human red blood cells. *J. Biol. Chem.* 264:5080–5088.

Papahadjopoulos, D., W. J. Vail, K. Jacobson, and G. Poste. 1975. Cochleate lipid cylinders: formation by fusion of unilamellar lipid vesicles. *Biochim. Biophys. Acta.* 394:483–491.

Prestwich, G. D. 1996. Touching all the bases—synthesis of inositol polyphosphate and phosphoinositide affinity probes from glucose. *Acc. Chem. Res.* 29:503–513.

Rittenhouse, S. E., and J. P. Sasson. 1985. Mass changes in myoinositol trisphosphate in human platelets stimulated by thrombin. Inhibitory effects of phorbol ester. *J. Biol. Chem.* 260:8657–8660.

Rupert, L. A. M., J. F. L. v. Breemen, E. F. J. v. Bruggen, J. B. F. N. Engberts, and D. Hoekstra. 1987. Calcium-induced fusion of didodecylphosphate vesicles: the lamellar to hexagonal II (HII) phase transition. *J. Membr. Biol.* 95:255–263.

Sugiura, Y. 1981. Structure of molecular aggregates of 1-(3-*sn*-phosphatidyl)-L-*myo*-inositol 3,4-bis(phosphate) in water. *Biochim. Biophys. Acta.* 641:148–159.

Surridge, C. D., and R. G. Burns. 1994. The difference in the binding of phosphatidylinositol distinguishes MAP2 from MAP2c and tau. *Biochem.* 33:8051–8057.

Thurston, V., R. Zinkowski, and L. Binder. 1996. Tau as a nucleolar protein in human nonneural cells in vitro and in vivo. *Chromosoma.* 105:20–30.

Wang, Y., P. A. Loomis, R. P. Zinkowski, and L. I. Binder. 1993. A novel tau transcript in cultured human neuroblastoma cells expressing nuclear tau. *J. Cell Biol.* 121:257–267.

Wilson, D. M., and L. I. Binder. 1995. *Mol. Biol. Cell.* 6:37a.

Yu, F. X., H. Q. Sun, P. A. Janmey, and H. L. Yin. 1992. Identification of a polyphosphoinositide-binding sequence in an actin monomer-binding domain of gelsolin. *J. Biol. Chem.* 267:14616–14621.